JACS
JOURNAL OF THE AMERICAN CHEMICAL SOCIETY

Article

pubs.acs.org/JACS

Type-II CdSe/CdTe Core/Crown Semiconductor Nanoplatelets

Silvia Pedetti,[†,‡] Sandrine Ithurria,[‡] Hadrien Heuclin,[†] Gilles Patriarche,[§] and Benoit Dubertret*[,‡]

[†]Nexdot, 10 rue Vauquelin, 75005 Paris, France

[‡]Laboratoire de Physique et d'Etude des Matériaux, ESPCI-ParisTech, PSL Research University, Sorbonne Université UPMC Univ Paris 06, CNRS, 10 rue Vauquelin, 75005 Paris, France

[§]Laboratoire Photonique et Nanostructures, CNRS, 91460 Marcoussis, France

Supporting Information

ABSTRACT: We have synthesized atomically flat CdSe/CdTe core/crown nanoplatelets (NPLs) with thicknesses of 3, 4, and 5 monolayers with fine control of the crown lateral dimensions. In these type-II NPLs, the charges separate spatially, and the electron wave function is localized in the CdSe core while the hole wave function is confined in the CdTe crown. The exciton's recombination occurs across the heterointerface, and as a result of their spatially indirect band gap, an important emission red shift up to the near-infrared region (730 nm) is observed with long fluorescence lifetimes that range from 30 to 860 ns, depending on the type of interface between the core and the crown. These type-II NPLs have a high quantum yield of 50% that can be further improved to 70% with a gradient interface. We have characterized these novel CdSe/CdTe core/crown NPLs using UV−vis, emission, and excitation spectroscopy, X-ray diffraction, energy-dispersive X-ray spectroscopy, and high-resolution transmission electron microscopy.

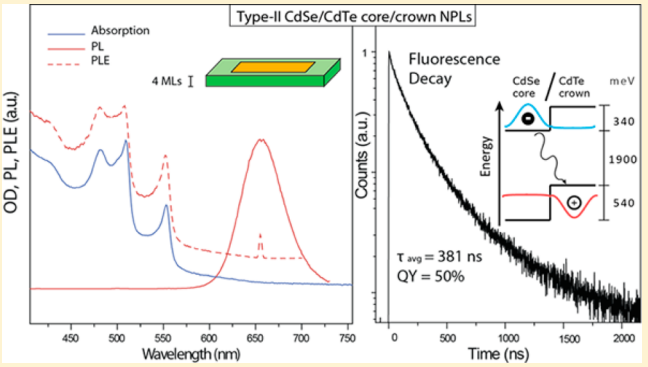

INTRODUCTION

The research on colloidal nanostructures has greatly expanded since the first synthesis of spherical semiconductor nanocrystals (NCs) with a narrow size distribution.[1] Today, not only the sizes of the NCs can be finely controlled,[2] but also their shapes.[3] Thus, nanorods,[4] nanowires,[5] and nanoplatelets,[6] with confinement of the exciton in three, two, or one dimension, respectively, have been synthesized. The improvement in colloidal syntheses has also led to the design of core/shell NC heterostructures[7] composed of different materials.[8,9] Depending on the alignment between the conduction and valence bands of the core and the shell, these core/shell NCs can behave as type-I or type-II heterostructures.[8,9] In type-I NCs, both electrons and holes wave functions are confined in the same material because of a wider band gap of either the core or shell material. In type-II core/shell NCs, the electron and holes wave functions are localized in different parts of the NC, resulting in efficient spatial separation of the charges and longer fluorescence lifetimes.

The first type-II colloidal quantum dots (CdTe/CdSe and CdSe/ZnTe) were synthesized in 2003.[10] Their emission wavelengths ranged between 700 and 1000 nm, with rather poor photoluminescence (PL) quantum yields (QYs) of 0−30%.[10−12] Several combinations of semiconductors for the core and shell materials have been tested ever since in order to improve the NCs' photophysical properties.[13] It has also been shown that the HOMO−LUMO energy gap of the core and the band gap alignment between the core and the shell, at the origin of the type-II behavior, can be finely tuned by changing the dimensions of the core or the shell of the NCs[14] or by controlling the compressive strain[15] induced by the shell on the core. Type-II NCs have been proposed for applications in photovoltaics,[16,17] light-emitting diodes (LEDs),[18] and lasing technologies.[19,20] Nonspherical type-II heterostructures have also been reported but to date have been limited to one-dimensional (1D) objects such as (Zn,Cd)Te/CdSe nanowires[21] and CdSe/CdTe nanorods.[22] To the best of our knowledge, there has been no report on two-dimensional (2D) type-II heterostructures.

During the past few years a new class of colloidal 2D materials, named nanoplatelets (NPLs),[6] nanoribbons,[23] quantum belts,[24] nanosheets,[25] or quantum disks,[26] has emerged. These 2D nanocrystals have unique optical properties such as sharp absorption and emission peaks, quasi-zero Stokes shifts, and short radiative fluorescence lifetimes.[27] Cadmium-based CdS,[27,28] CdSe,[29] and CdTe[30] NPLs have been synthesized with control of their thickness with atomic precision and wide modulation of their lateral extension. Recently, core/shell NPLs have been synthesized.[31,32] Quasi-type-II CdSe/CdS core/shell NPLs have been obtained with QYs as high as 80%.[33] Moreover, some novel 2D CdSe/CdS

Received: September 9, 2014
Published: October 22, 2014

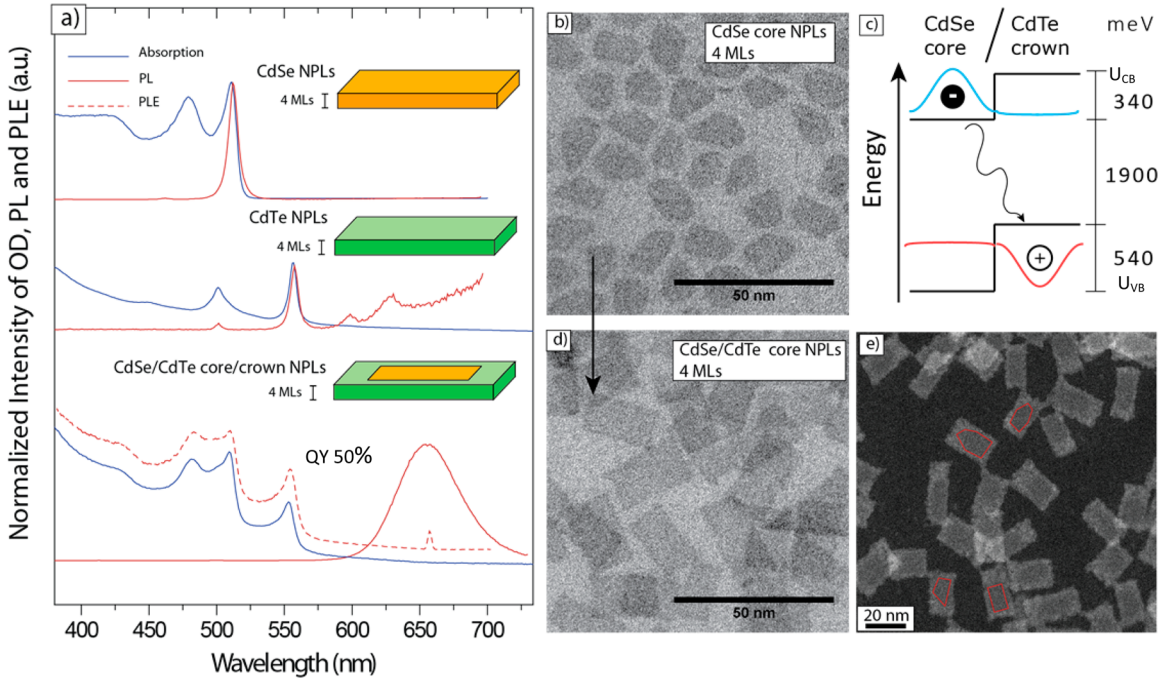

Figure 1. (a) Absorption, photoluminescence (PL), and PL excitation (PLE) spectra normalized at the first exciton peak for 4 ML thick (top) CdTe NPLs, (middle) CdSe NPLs, and (bottom) CdSe/CdTe core/crown NPLs. (b, d) TEM images of 4 ML thick CdSe core NPLs and 4 ML thick CdSe/CdTe core/crown NPLs, respectively. (c) Schematic representation of band alignment in CdSe/CdTe semiconductors showing the indirect charge recombination. Energy values refer to 4ML thick CdSe/CdTe core/crown NPLs. (e) HAADF-STEM image of CdSe/CdTe core/crown NPLs. Guidelines for the eyes correspond to the core region.

core/crown NPLs have been grown by lateral extension of CdSe NPLs with a CdS crown.[34,35] These heterostructures behave as exciton concentrators because of the quasi-type-II band alignment and the strong exciton binding energy.[35] NPLs have also shown promising performances when used in devices.[36,37]

In this paper, we present the first examples of type-II CdSe/CdTe core/crown NPLs. Starting from CdSe NPLs, we extended them laterally with a CdTe crown. We synthesized three different populations of type-II core/crown NPLs with thicknesses of 3, 4, and 5 monolayers (MLs). The CdSe/CdTe core/crown NPLs are atomically flat with core and crown domains that have exactly the same number of MLs. We performed structural characterization of the core, the crown, and their interface and studied the effects of their dimension/composition on the optical properties of the NLPs. The PL emission of the CdSe/CdTe NPLs can be tuned up to the near-infrared region with fluorescence lifetimes of the order of 100 ns and QYs of up to 60%.

RESULTS AND DISCUSSION

The synthesis of CdSe/CdTe core/crown NPLs involves two steps. During the first step, CdSe core NPLs are prepared by colloidal synthesis and purified from the reaction mixture as described in the literature.[38] These NPLs possess a zinc blende crystallographic structure with external facets that are perpendicular to the [001] direction. The largest facets of CdSe NPLs are cadmium-rich surfaces passivated by the carboxylate groups of the oleate ligands. The characteristic optical features of these 4 ML thick CdSe NPLs are reported in Figure 1a (top). The first excitonic peak relative to the heavy hole to electron transition is observed at 511 nm, and the emission due to the exciton recombination is at 512 nm with almost no Stokes shift and with a full width at half-maximum (FWHM) of 10 nm. In Figure 1b, a transmission electron microscopy (TEM) image shows the morphology of these CdSe NPLs with average lateral dimensions of 10 nm × 14 nm. The second step of the synthesis consists of the epitaxial lateral extension of these CdSe core NPLs with a crown of CdTe. Generally, CdSe core NPLs were dispersed in a non-coordinating solvent such as 1-octadecene (ODE) with a cadmium salt (cadmium propionate, $Cd(Prop)_2$) and an organic ligand with a long aliphatic chain (oleic acid, OA). The reaction temperature was then increased to 235 °C, and 1 M trioctylphosphine telluride (TOPTe) was continuously injected. The CdSe/CdTe core/crown NPLs were separated from the reaction mixture by selective precipitation and then observed by TEM. In Figure 1d, a TEM image of CdSe/CdTe core/crown NPLs with a thickness of 4 MLs is presented. It shows larger NPLs with a rectangular shape and average lateral dimensions of 12 nm × 20 nm. Optical measurements (absorption, emission, and excitation spectra) of the CdSe/CdTe core/crown NPLs are reported in Figure 1a (bottom). The absorption spectrum is a combination of the absorption spectra of CdSe and CdTe. The excitonic peaks at 480 and 511 nm are assigned to the light hole−electron (lh−e) and heavy hole−electron (hh−e) transitions in CdSe NPLs. The peak recorded at 554 nm is attributed to the heavy hole−electron transition in CdTe NPLs. This assignment is consistent with the absorption spectrum reported for 4 ML thick CdTe NPLs (Figure 1a middle), which presents two excitonic transitions at 500 nm (lh−e) and 556 nm (hh−e).[30] The PL spectrum shows a maximum of the emission peak strongly shifted toward low energy, at 656 nm, with a FWHM of 54 nm. The photoluminescence excitation (PLE) spectrum (red dashed line in Figure 1a bottom) obtained at the maximum of emission

dx.doi.org/10.1021/ja509307m | J. Am. Chem. Soc. 2014, 136, 16430−16438

is similar to the absorption spectrum. The purity of the as-synthesized NPLs is thus spectrally confirmed, and we can exclude the possibility that the excitonic peaks characteristic of CdTe NPLs are due to secondary nucleation of CdTe NPLs during the reaction. Recently CdSe/CdS core/crown NPLs were prepared, and their spectra exhibit specific absorption features from both CdSe and CdS NPLs with the same number of MLs.[35] In CdSe/CdS core/crown NPLs the PL emission is only slightly red-shifted with respect to that of CdSe core NPLs with a FWHM of <15 nm. This results from the strong exciton binding energy of flat CdSe/CdS core/crown NPLs, in which the CdS crown behaves as an exciton funnel toward the CdSe core. On the contrary, for the CdSe/CdTe core/crown NPLs presented in this work, the charge carriers are separated between the core and the crown, as expected for a CdSe/CdTe core/shell structure,[39] which have band offsets of 0.42 and 0.57 eV for the conduction and valence bands, respectively, in the bulk materials.[40] The schematic representation in Figure 1c describes the band-edge alignment for 4 ML thick CdSe/CdTe core/crown NPLs, whose UV–vis and PL spectra are reported in Figure 1a (bottom). The energy differences between the valence and conduction bands reported in Figure 1c were calculated using the absorption and emission energies. In these hetero-NPLs, the charges are separated, with the elctron wave function localized in the CdSe core and the hole in the CdTe crown. As a result, the PL emission due to the radiative recombination of the exciton is red-shifted compared with both 4 ML thick CdSe and CdTe NPLs. The FWHM of the PL peak is larger than those of bare CdSe and CdTe NPLs (156 meV vs 50 and 40 meV, respectively). The broadening of the band width is a common feature of type-II nanocrystals.[10,41] It results from the combined effect of the inhomogeneous broadening, correlated to the size dispersion of the NCs, and of the homogeneous broadening, which depends on the exciton dephasing and represents the intrinsic transition line width. The great increase in the FWHM observed for the CdSe/CdTe core/crown NPLs cannot be explained only by the inhomogeneity of the sample since, as shown in Figure S1 in the Supporting Information, the excitation spectra at different wavelengths (λ_1 = maximum of emission, $\lambda_{2,3}$ = maximum of emission ± FWHM/2) are identical. Moreover the confinement direction (i.e., the thickness) remains precisely controlled during the crown growth. We thus attribute the significant FWHM increase for type-II NPLs mainly to homogeneous broadening. It has been demonstrated that stronger polarization of the exciton with separation of the charges results in an increase in the optical phonon coupling.[42,19] For type-I NPLs (bare CdSe, CdS, and CdTe), the exciton local charge is neutral and the polar coupling of the exciton with the optical phonons is weak. On the contrary, in our type-II NPLs the electrons and holes are well-separated and the coupling with the lattice vibrations is stronger.[43] This results in an increase in the line width. Additionally, it is possible to consider the Marcus theory[44] for photoinduced charge separation in nanocrystalline heterostructures. It has been shown that for type-II CdSe/CdTe heteronanorods the free energy of the charge-transfer state is displaced compared with the free energy of the exciton state. Indeed, it results that the homogeneous line broadening observed for the charge-transfer emission peak is related to the reorganization energy of the environment to stabilize the charge-transfer state and thus a larger dipole.[45]

Usually, type-II NCs are limited by low QYs since fast nonradiative processes dominate over the slower indirect

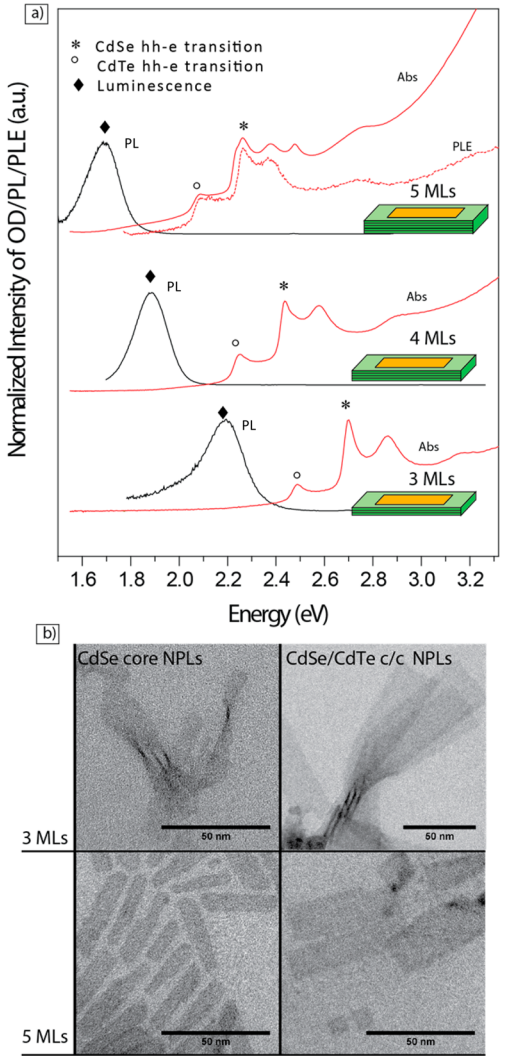

Figure 2. (a) Absorption, PL, and PLE spectra of CdSe/CdTe core/crown NPLs of different thicknesses: (top) 5 MLs, (middle) 4 MLs, and (bottom) 3 MLs. The heavy hole–electron transitions are marked with circles for CdTe and asterisks for CdSe. (b) On the left are shown TEM images of CdSe core NPLs with thicknesses of (top) 3 MLs and (bottom) 5 MLs. The NPL lateral sizes are respectively 60 nm × 10 nm (3 MLs) and 40 nm × 8 nm (5 MLs). On the right are shown TEM images of same CdSe NPLs with CdTe crowns.

exciton recombination.[13] However, highly efficient type-II NCs with QYs of up to 70% have recently been reported.[12,21,41,46] In the case of 4 ML thick CdSe/CdTe core/crown NPLs, the QY is close to 50%. Such a high value is probably due to the quality and the composition of the core–crown interface, as will be discussed later.

The spatial localization of the core and crown domains can be visualized with the high-angle annular dark-field scanning TEM (HAADF-STEM) image in Figure 1e. The CdTe crown region appears brighter than the CdSe core because of its higher electron density. The CdSe core NPLs possess a rather irregular morphology (Figure 1b), but we can observe regular rectangles as the CdSe/CdTe core/crown NPLs form. The core/crown geometry is further evidenced using the intensity profile of a high-resolution HAADF-STEM image of a single NPL (Figure S2). The profile shows a single NPL with a lateral size of 15.1 nm with a 5.2 nm wide central region of lower intensity corresponding to the CdSe core and two external

dx.doi.org/10.1021/ja509307m | J. Am. Chem. Soc. 2014, 136, 16430–16438

regions with widths of about 5 nm and higher intensity corresponding to the CdTe crown.

We then explored the possibility of synthesizing CdSe/CdTe core/crown NPLs with different thicknesses. We synthesized 3 and 5 ML thick CdSe core NPLs (Figure 2b), and after washing, we extended them with CdTe by the injection of TOP into a mixture of ODE, $Cd(Prop)_2$, metallic Te, OA, and CdSe core NPLs. The TOP injection was performed at 200 °C for the 3 ML thick CdSe NPLs and at 240 °C for the 5 ML ones.

Figure 2a shows the absorption and emission spectra as a function of the energy for 3, 4, and 5 ML thick CdSe/CdTe core/crown NPLs. In each absorption spectrum, the CdSe and CdTe hh−e transitions are clearly visible. The lh−e transition is also visible in the case of CdSe. The emission peaks for 3, 4, and 5 ML thick CdSe/CdTe core/crown NPLs are at 2.2, 1.9, and 1.7 eV respectively, with FWHMs of 190, 156, 160 meV.

We next analyzed the effect of the CdTe crown growth on the optical properties of 4 ML thick CdSe/CdTe core/crown NPLs. The synthesis was performed by injecting 50 μmol of 1 M TOPTe in 2.5 min at 235 °C into a reaction mixture containing square CdSe core NPLs, OA, and $Cd(Prop)_2$ (0.5 mmol) in the ratio 1.5:1 in ODE. The absorption and emission spectra recorded between 5 s and 10 min after the beginning of the TOPTe injection are reported in Figure 3a. The volume of the CdTe crown is related to the intensity of the CdTe peak at 550 nm (marked by an asterisk in Figure 3a). At the early stage of the reaction (between 5 s and 1.5 min), the absorption in that region is very weak, and it is only after 10 min that the absorption due to the crystalline CdTe crown is clearly visible. On the contrary, the luminescence of the CdSe/CdTe NPLs changes radically as soon as the tellurium precursor is injected. Five seconds after the onset of the injection, two emission peaks are already visible: a sharp one at 510 nm due to the CdSe core NPLs and another broader one at ca. 630 nm (1.97 eV) (Figure 3a). After 30 s, the peak at 510 nm has disappeared, and only a well-defined peak at 640 nm remains. This means that the overlap of the carriers' wave functions is only partial across the heterointerface between the core and the small crown. In the successive spectra recorded after 1.5 and 10 min, the maxima of the emission spectra are red-shifted by 30 nm while the line width remains unchanged. The spectrum corresponding to the final product, at t = 15 min, is reported in Figure S3. The appearance of the peak at ∼630 nm even 5 s after the beginning of the reaction shows that as soon as the CdTe starts to grow at the edges of the CdSe NPLs, a type-II interface with charge separation is formed. This charge separation even for very small CdTe crowns can be qualitatively understood if we compare the energies that impact on the exciton. On the one hand, the binding energy of the exciton, on the order of 300 meV,[47,48] tends to keep the electron and the hole together. On the other hand, the band alignment tends to spatially split the charges, with the hole in the CdTe and the electron in the CdSe. For the 4 ML thick NPLs, 5 s after the injection of tellurium, the absorption energy of the first exciton transition in the CdSe core is 2.43 eV, and the radiative exciton recombination occurs at 1.97 eV. The energy difference, 460 meV, gives the valence band offset (Figure 1c), which is greater than the exciton binding energy. This explains why the charges are completely separated even for very tiny CdTe crowns.

When the charges are separated, another parameter can impact the excitonic transition: the lateral confinement of the charges when the CdTe crown is small compared to the Bohr radius of the hole. We have approximated the value of the Bohr

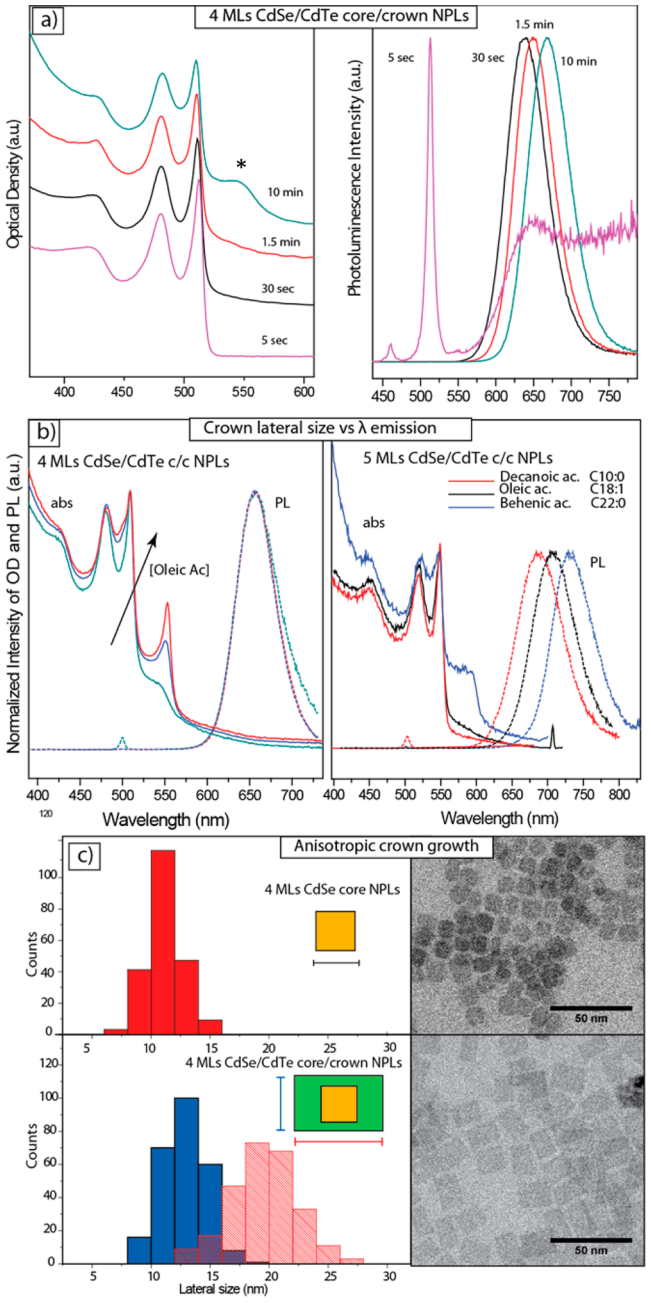

Figure 3. (a) Absorption (left) and emission (right) spectra of CdSe/CdTe NPLs during the growth of the CdTe crown. (b) On the left are shown absorption and emission spectra (solid and dashed lines, respectively) of 4 ML thick CdSe/CdTe core/crown NPLs synthesized with different concentrations of oleic acid: 0.15, 0.22, and 0.4 M. On the right are shown absorption and emission spectra (solid and dashed lines, respectively) of 5 ML thick CdSe/CdTe core/crown NPLs prepared using aliphatic chains of different lengths. (c) Size distributions of the lateral dimensions of 4 ML thick CdSe/CdTe core/crown NPLs prepared using square 4 ML thick CdSe core NPLs.

radius for the hole, a_h(CdTe), as 1.12 nm. This suggests that after a CdTe crown extension of few nanometers, the hole is confined only in the direction of the thickness. The suppression of the hole lateral confinement as the CdTe crown grows explains the red shift of the PL observed in Figure 3a (right) and its quick saturation at 656 nm.

We also explored the influence of the concentration and the length of the aliphatic chain of the carboxylate ligands on the

dx.doi.org/10.1021/ja509307m | J. Am. Chem. Soc. 2014, 136, 16430−16438

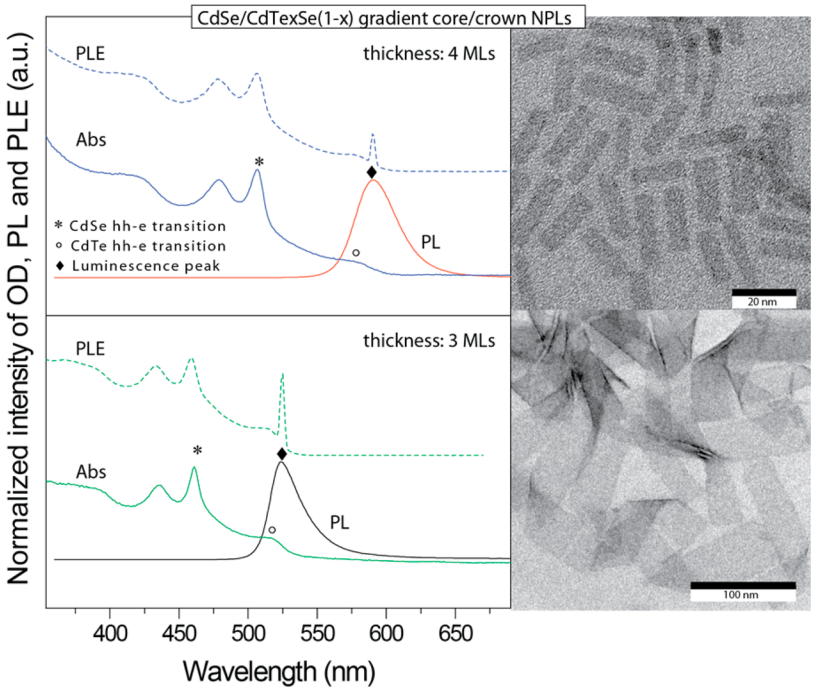

Figure 4. (left) UV−vis, PL, and PLE spectra and (right) TEM images of CdSe/CdTe$_x$Se$_{(1-x)}$ gradient core/crown NPLs with thicknesses of (top) 4 MLs and (bottom) 3 MLs. The lateral extensions are on average 20 nm × 5 nm for the thicker NPLs and 200 nm × 50 nm for the thinner NPLs.

growth of the CdTe crown. First, we note that all of the syntheses of heteronanoplatelets were performed with an excess of Cd precursor, so the Te precursor was the limiting reagent for the crown growth (as better shown in Figure S4). Figure 3b (left) compares the absorption and emission spectra for three different batches of 4 ML thick CdSe/CdTe core/crown NPLs prepared using the same amount of Te but varied amounts of OA. The syntheses were performed by continuously adding TOP and OA in ODE into a mixture containing CdSe core NPLs, metallic Te, and Cd(Prop)$_2$ in ODE. We observed that high concentrations of OA give core/crown NPLs with a higher excitonic peak for CdTe (at 554 nm) and thus more extended CdTe crowns, as confirmed by the TEM images (Figure S5). As expected, the luminescence peaks of the NPL populations are all similar, regardless of the OA concentration we tested. This confirms that all of these NPLs have a crown large enough so that the hole is not confined laterally.

As in the case of CdSe/CdS core/crown NPLs,[35] the crown extension is strongly correlated to the thickness of the core NPLs: the use of thinner CdSe NPLs results in faster lateral extension with CdTe. For 3 ML thick CdSe NPLs, the extension of CdTe can largely overcome the CdSe core dimensions, resulting in core/crown NPLs exhibiting greater absorption of CdTe than CdSe (Figure S6). For the thicker 4 ML population, the lateral growth is in competition with the secondary nucleation of 3 ML thick CdTe NPLs, which is thermodynamically more favorable. The secondary nucleation is easily separated by selective precipitation, as the lateral sizes of the two products differ by 1 order of magnitude (Figure S7). Secondary nucleation can be avoided if higher concentrations of 4 ML thick core NPLs are used. In the case of 5 ML thick CdSe core NPLs, CdTe crown growth is difficult, and the protocol had to be adapted. To perform CdTe lateral extension on 5 ML thick CdSe NPLs, we had to increase the length of the aliphatic part of the carboxylic acid ligand, a technique that was previously used to grow thick CdS NPLs.[28] As we increased the length of the aliphatic chain from 10 (decanoic acid) to 22 (behenic acid), we observed stronger absorption due to the CdTe crown growth and a red shift of the emission peak from 690 to 730 nm (Figure 3b), demonstrating the growth of an extended CdTe crown on the 5 ML thick CdSe core NPLs.

We also analyzed the morphology of the CdSe NPLs before and after the extension with CdTe. As pointed out in Figure 1d,e, the morphology of the 4 ML thick CdSe/CdTe core/crown NPLs is more regular than that of CdSe core NPLs. Figure 3c shows the distributions of the lateral dimensions of the CdSe core NPLs with square morphology before CdTe crown growth and the CdSe/CdS core/crown NPLs after CdTe crown growth. Surprisingly, the square shape (10 nm × 10 nm) of the CdSe core NPLs becomes rectangular (12 nm × 18 nm) after crown growth. This anisotropy induced during the crown formation in spite of the cubic crystal structure is similar to the anisotropies observed during the lateral extension of CdSe NPLs[29] and could arise from slightly different facet energies of the CdSe core NPLs.

We analyzed the optical properties of CdSe/CdTe core/crown NPLs when the interface between the core and crown is a gradient. This analysis was motivated by two points: to get higher QYs (as already observed for CdS/ZnSe quantum dots[12,49]) and to suppress Auger recombination for better photostability.[50] CdSe/CdTeSe core/crown NPLs with a gradient composition at the interface were obtained by the injection of Cd and Te precursors into the solution of CdSe core NPLs during their formation. Depending on the time delay between nucleation of the CdSe NPLs and the crown extension, unreacted Se precursor remains in the reaction mixture and can be incorporated into the crown. In Figure 4, typical optical features of these CdSe/CdTe$_x$Se$_{(1-x)}$ core/crown NPLs with thicknesses of 3 and 4 MLs are reported. The asterisks indicate the first excitonic transition in the CdSe cores, which appear at 462 and 507 nm for the 3 and 4 ML thick CdSe/CdTeSe core/crown NPLs, respectively. The open

dx.doi.org/10.1021/ja509307m | J. Am. Chem. Soc. 2014, 136, 16430−16438

circles indicate the excitonic peak of the crown. For pure 3 and 4 ML thick CdTe NPLs, the first excitonic peaks are at 500 and 556 nm, respectively. In these new types of hetero-NPLs, the absorptions of the crowns are red-shifted to 516 and 576 nm for the 3 and 4 ML thick NPLs, respectively. This red shift compared with pure CdTe is due to the alloyed composition of the crown, which results in optical bowing of the band gap.[51,52] The PL peaks, marked by diamonds, are located at 524 and 590 nm for 3 and 4 ML thick NPLs, respectively. The band edge emissions recorded for these hetero-NPLs prepared in situ are at higher energies as a consequence of the gradient interface between the pure core and the alloyed crown. The QY of the CdSe/CdTeSe gradient core/crown NPLs is to up to 70%, better than that of the corresponding CdSe/CdTe core/crown NPLs described previously.

We also characterized the structure of abrupt CdSe/CdTe core/crown NPLs. First of all, the chemical composition of the core/crown NPLs was investigated by energy-dispersive X-ray spectroscopy (EDX). In Figure 5A we report a representative example of EDX analysis of a single NPL, where the chemical composition was analyzed at several points along the longer (blue line) and shorter (green line) lateral dimensions. The EDX probe step size was 2 nm, and the resolution of the probe

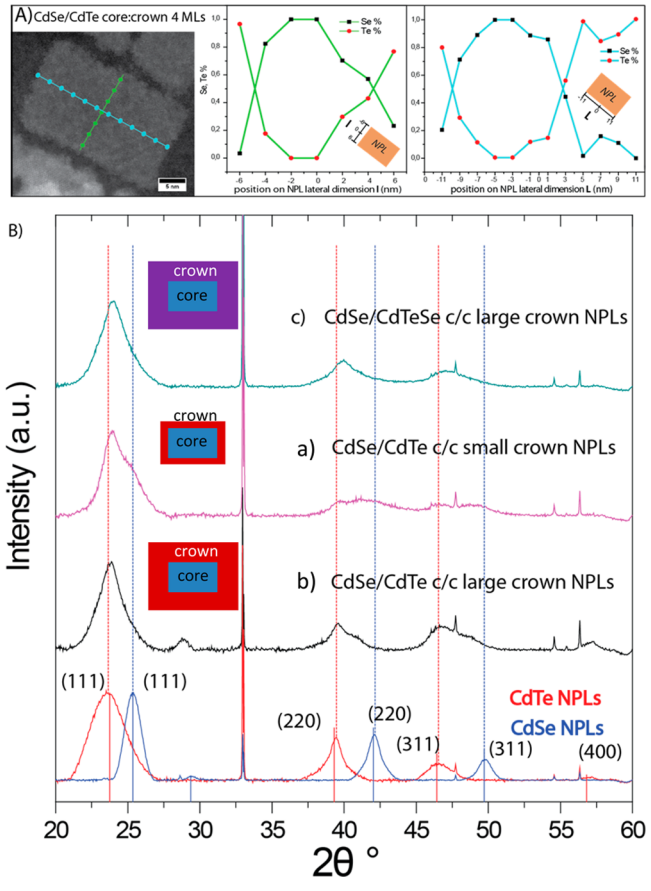

Figure 5. (A) Atomic-resolution HAADF-STEM image of a single CdSe/CdTe core/crown NPL, with green and blue lines showing the EDX probe positions. The compositions in selenium and tellurium, normalized to the total anionic composition, are reported in the graphs at the right. (B) Powder X-ray diffractograms of core/crown NPLs. The reference peaks for CdSe and CdTe (vertical lines) and the diffractograms of bare CdTe and CdSe NPLs are reported at the bottom.

was ca. 1 nm, as shown in Figure S8. This experiment clearly points out a core/crown structure with an internal core of CdSe and an external crown of CdTe mainly extended along the longer lateral dimension. The absence of abrupt and well-defined interfaces as we observed in the case of CdSe/CdS core/crown NPLs is probably due to partial dissolution of the core CdSe NPLs in the presence of TOP at the beginning of the injection of TOPTe. We have indeed observed that CdSe NPLs in the presence of an excess of TOP can completely dissolve, while the dissolution is suppressed when an excess of cadmium salt is added (Figure S9), as it is the case during the extension of the CdTe crown.

We also analyzed different CdSe/CdTe core/crown NPLs by powder X-ray diffraction. In Figure 5B, diffractograms for the following samples are presented: (a) 5 ML thick CdSe/CdTe core/crown NPLs with a very small CdTe crown equal to 0.2 times the CdSe core volume; (b) 4 ML thick CdSe/CdTe core/crown NPLs synthesized such that the CdTe crown volume equals 1.2 times the CdSe core volume; and (c) CdSe/CdTeSe core/alloyed-crown NPLs, for which spectroscopic data and a TEM image are shown in Figure S10a. We have also reported at the bottom of Figure 5B the diffractograms of zinc blende CdSe and CdTe NPLs and the references for the bulk cubic CdSe and CdTe (solid vertical lines). Interestingly, the diffractogram (a) (small crown) is a mixture of the pure CdSe and pure CdTe diffractograms. For diffractogram (b), we mostly observe the peaks coming from the CdTe crown. For the family of planes (220) and (311), the shoulders at larger angles are probably due to dilatation of the CdSe core. Finally, in diffractogram (c) corresponding to CdSe/CdTeSe core/alloyed-crown NPLs, a sample similar to that in (b) except for the composition of the crown, the peak coming from the crown is shifted to higher angles compared with pure CdTe. From Vegard's law,[53] for the crystallographic family plane (220) the composition of the crown was estimated as $CdTe_{0.7}Se_{0.3}$.

In type-II NCs, the overlap of the electron and hole wave functions is strongly reduced. This results in long fluorescence lifetimes and often low QYs. These two parameters, however, depend strongly on the interface between the core and the shell (abrupt, alloyed, or gradient) and on the quality of the interface (defects). We measured the fluorescence lifetimes and QYs (calculated using a reference fluorophore as described in the Supporting Information) of four different CdSe/CdTe core/crown NPLs (Figure 6a and Table 1). The QY is better for CdSe/CdTeSe core/alloyed-crown NPLs (>60% to 73%) than for CdSe/CdTe core/crown NPLs (<10% for the 5ML ones and 46% for the 4 ML ones). The positive effect of alloyed or gradient interfaces on type-II core/shell NCs has already been observed for spherical quantum dots.[49,54] The low QY for the 5 ML thick CdSe/CdTe NPLs is probably due to defects at the interface between the core and the crown, although this hypothesis is hard to test.

In spite of their low QY, the 5 ML thick CdSe/CdTe NPLs have the longest fluorescence lifetime, with an averaged lifetime (τ_{avg}) equal to 860 ns. For the 4 ML thick NPLs, τ_{avg} = 381.4 ns, which is 2 orders of magnitude longer than that of bare CdSe NPLs (which is a few nanoseconds at room temperature). The decays are multiexponential with important slow components (see Figure S11). These decays are longer than those usually reported for other type-II NCs, such as spherical CdTe/CdSe quantum dots and CdTe/CdSe nanowires (τ_{avg} = 100−350 ns),[12,21,55] with the exception of CdSe/CdTe collinear quantum rods[56] (0.745−1.821 μs) and CdSe/CdTe

dx.doi.org/10.1021/ja509307m | J. Am. Chem. Soc. 2014, 136, 16430−16438

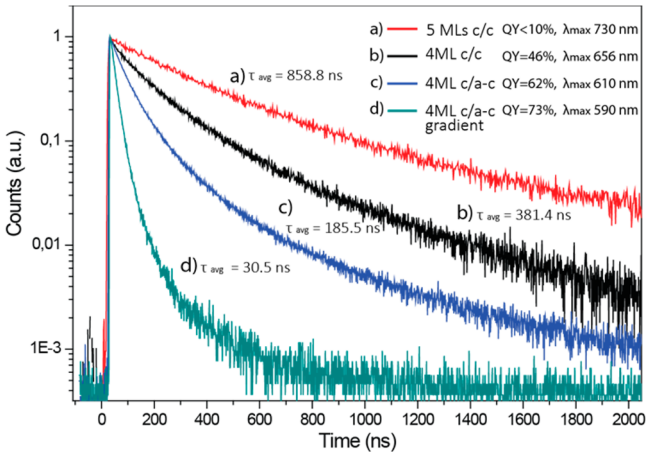

Figure 6. PL decays and associated lifetimes of CdSe/CdTe core/crown NPLs: (a) 5 ML thick CdSe/CdTe core/crown NPLs; (b) 4 ML thick CdSe/CdTe core/crown NPLs; (c) 4 ML thick CdSe/CdTeSe core/alloyed-crown NPLs with a sharper interface; (d) 4 ML thick CdSe/CdTeSe core/alloyed-crown NPLs with a gradient interface.

anisotropic hetero-NCs (390−715 ns).[41] When the interface is alloyed, shorter fluorescence lifetimes are observed (τ_{avg} = 185.5 ns), but the shortest lifetimes (τ_{avg} = 30.5 ns) are observed for gradient interfaces (optical features corresponding to the core/crown NPLs with the decay curves shown in Figure 6c,d are reported in Figure S10b,c). These shorter fluorescence lifetimes, combined with the higher QYs, confirm that for these 2D systems the interface plays a key role in the band alignment. The wave function overlap increases and the probability of radiative decay rises, proving the transition toward a quasi-type-II carrier localization regime.[41] Finally, the high tunability of the fluorescent lifetimes in these type-II structures should make them model systems when a long lifetimes and high QYs are needed, as is the case in lasers.

CONCLUSION

We have presented a novel class of type-II 2D nanocrystals: CdSe/CdTe core/crown NPLs. The synthesis was investigated in order to gain control of the lateral crown extension and the thickness uniformity. CdSe/CdTe core/crown NPLs with thicknesses of 3, 4, 5 MLs were synthesized and optically and structurally characterized. For the first time, to the best of our knowledge, we obtained atomically flat NPLs that present spatial separation of charges with the appearance of typical type-II features: important red shifts of the fluorescence emission up to the near-infrared, with the electron wave function localized in the CdSe core and the hole wave function in CdTe crown, and longer lifetime decays. Surprisingly, the QYs of the type-II 2D NPLs was high (up to 50%) and could be further improved to up to 70% by the formation of a gradient heterointerface through in situ crown growth. Moreover the long emission decays measured suggest potential applications in lasing technologies. This extension of core/crown NPLs to type-II structures highlights and confirms the importance of the interface composition in the band alignment and thus the optical properties of the core/shell structures. It also provides a synthetic route for the synthesis of type-II NPLs with high QYs, long fluorescence lifetimes, and emission wavelengths tunable from the visible to the near-IR.

METHODS AND MATERIALS

Chemicals. The following chemicals were obtained commercially: cadmium acetate dihydrate ($Cd(OAc)_2{\cdot}2H_2O$, 98%, Sigma-Aldrich), Se powder (99.99%, Strem Chemicals), 60 mesh Te powder (99.999%, Strem Chemicals), OA (90%, Aldrich), TOP (90%, Sigma-Aldrich), decanoic acid (98.0%, Sigma), behenic acid (99.0%, Fluka), *n*-hexane (98%, VWR), ethanol (98%, VWR), and ODE (90%, Aldrich). Cadmium myristate ($Cd(Myr)_2$)[57] and $Cd(Prop)_2$[58] were synthesized following reported procedures.

Preparation of 4 ML Thick CdSe NPLs. In a 100 mL three-neck flask, 340 mg of $Cd(Myr)_2$ (0.6 mmol) and 24 mg of Se powder (0.3 mmol) in 30 mL of ODE were mixed. The mixture was degassed under vacuum at room temperature for 20 min, and then, under an Ar flow, the temperature was set at 240 °C. When the temperature reached 205 °C, 80 mg of $Cd(OAc)_2$ (0.3 mmol) was swiftly introduced into the flask. After 12 min, the reaction was quenched by the addition of 2 mL of OA, and the mixture was rapidly cooled to room temperature. The NPLs were purified by selective precipitation upon addition of 30 mL of hexane and 30 mL of ethanol followed by centrifugation at 6000 rpm for 10 min. Then the supernatant was discarded, and the precipitate was redispersed in 10 mL of hexane.

Synthetic procedures for 3 and 5 ML thick CdSe NPLs are reported in the Supporting Information.

Preparation of 4 ML Thick CdSe/CdTe Core/Shell NPLs. The previously prepared 4 ML thick CdSe NPLs (4 mL) were precipitated with ethanol, resuspended in 6 mL of ODE, and transferred into a 25 mL three-neck flask. OA (238 μL, 0.75 mmol) and $Cd(Prop)_2$ (130 mg, 0.5 mmol) were added, and the mixture was degassed under vacuum for 30 min. Then the temperature was increased under an Ar flow, and when it reached 235 °C, a solution of 50 μL of 1 M TOPTe in 1 mL of ODE was added at an injection rate of 24 mL/h. After 15 min, 1 mL of OA was swiftly added, and the mixture was cooled to room temperature. The core/crown NPLs were purified by selective precipitation with hexane and ethanol followed by centrifugation at 5000 rpm for 10 min. The CdSe/CdTe core/crown NPLs were separated from CdTe NLs formed by homogeneous secondary nucleation by centrifugation at 3000 rpm in hexane for 10 min.

Preparation of 4 ML Thick CdSe/CdTeSe Core/Alloyed-Crown NPLs. In a 50 mL three-neck flask, 85 mg of $Cd(Myr)_2$ (0.15 mmol) and 6 mg of Se powder (0.075 mmol) were added to 10 mL of ODE. The mixture was degassed at room temperature for 30 min, and then, under an Ar flow, the temperature was set at 230 °C. When the temperature reached 200 °C, 20 mg of $Cd(OAc)_2$ (0.075 mmol) was swiftly added into the flask. Then at 230 °C (3 min after the acetate addition), addition of 130 mg of $Cd(Prop)_2$ (0.5 mmol) and 13 mg of Te powder (0.1 mmol) was performed, followed by continuous injection of a solution composed of 355 μL (1.12 mmol) of OA and 50 μL (0.1 mmol) of TOP in 3 mL of ODE at an injection rate of 36 mL/h. After 30 min, 1 mL of OA was added, and the temperature was rapidly lowered. CdSe/CdTeSe NPLs were purified by addition of 10

Table 1. PL, QY, and Half-Life Data for the Type-II Core/Crown NPLs Reported in Figure 6

	(a) 5 ML thick core/crown	(b) 4 ML thick core/crown	(c) 4 ML thick core/alloyed-crown	(d) 4 ML thick gradient core/alloyed-crown
PL (nm)	730	656	610	590
QY[a]	<10%	46%	62%	73%
τ_{avg} (ns)	858.8	381.4	185.5	30.5

[a]The fluorophore used for QY measurements was rhodamine 6G.

mL of hexane and 5 mL of ethanol followed by centrifugation at 5000 rpm for 10 min. The precipitate was finally redispersed in 5 mL of hexane.

Synthetic procedures for 3 and 5 ML thick CdSe/CdTe core/crown NPLs are reported in the Supporting Information.

Material Characterization. UV−vis absorption spectra and PL and PLE spectra were acquired using Varian Cary 5E and Horiba Jobin-Yvon Fluoromax-3 spectrometers, respectively. The PL decay was recorded using an Edinburgh Instruments F900 spectrometer. X-ray diffraction was performed on a Philipps X'pert system using the Cu Kα line. TEM images were acquired using a JEOL 2010 microscope and a JEOL 2200 FS microscope in HAADF-STEM configuration. EDX analyses were performed with a probe current of 150 pA and a probe size of 0.12 nm (FWHM), and the half-angle of convergence of the probe was 30 mrad.

■ ASSOCIATED CONTENT

Supporting Information

Additional information on sample characterization, methods, and materials. This material is available free of charge via the Internet at http://pubs.acs.org.

■ AUTHOR INFORMATION

Corresponding Author

benoit.dubertret@espci.fr

Notes

The authors declare no competing financial interest.

■ ACKNOWLEDGMENTS

We are grateful to Alexander Efros for stimulating discussions and critical reading of the manuscript; we thank B. Nadal for fruitful discussions and X. Xu for her help during the TEM imaging.

■ REFERENCES

(1) Murray, C. B.; Norris, D. J.; Bawendi, M. G. *J. Am. Chem. Soc.* **1993**, *115*, 8706.

(2) Park, J.; An, K.; Hwang, Y.; Park, J.-G.; Noh, H.-J.; Kim, J.-Y.; Park, J.-H.; Hwang, N.-M.; Hyeon, T. *Nat. Mater.* **2004**, *3*, 891.

(3) Yin, Y.; Alivisatos, A. P. *Nature* **2005**, *437*, 664.

(4) Peng, X. G.; Manna, L.; Yang, W. D.; Wickham, J.; Scher, E.; Kadavanich, A.; Alivisatos, A. P. *Nature* **2000**, *404*, 59.

(5) Yu, H.; Li, J.; Loomis, R. A.; Gibbons, P. C.; Wang, L.-W.; Buhro, W. E. *J. Am. Chem. Soc.* **2003**, *125*, 16168.

(6) Ithurria, S.; Dubertret, B. *J. Am. Chem. Soc.* **2008**, *130*, 16504.

(7) Hines, M. A.; Guyot-Sionnest, P. *J. Phys. Chem.* **1996**, *100*, 468.

(8) Reiss, P.; Protière, M.; Li, L. *Small* **2009**, *5*, 154.

(9) de Mello Donegà, C. *Chem. Soc. Rev.* **2011**, *40*, 1512.

(10) Kim, S.; Fisher, B.; Eisler, H.-J.; Bawendi, M. *J. Am. Chem. Soc.* **2003**, *125*, 11466.

(11) Yu, K.; Zaman, B.; Romanova, S.; Wang, D.-s.; Ripmeester, J. A. *Small* **2005**, *1*, 332.

(12) Chin, P. T. K.; de Mello Donegá, C.; van Bavel, S. S.; Meskers, S. C. J.; Sommerdijk, N. A. J. M.; Janssen, R. A. J. *J. Am. Chem. Soc.* **2007**, *129*, 14880.

(13) Lo, S. S.; Mirkovic, T.; Chuang, C.-H.; Burda, C.; Scholes, G. D. *Adv. Mater.* **2011**, *23*, 180.

(14) Balet, L. P.; Ivanov, S. A.; Piryatinski, A.; Achermann, M.; Klimov, V. I. *Nano Lett.* **2004**, *4*, 1485.

(15) Smith, A. M.; Mohs, A. M.; Nie, S. *Nat. Nanotechnol.* **2009**, *4*, 56.

(16) Zhong, H.; Zhou, Y.; Yang, Y.; Yang, C.; Li, Y. *J. Phys. Chem. C* **2007**, *111*, 6538.

(17) Tong, S. W.; Mishra, N.; Su, C. L.; Nalla, V.; Wu, W.; Ji, W.; Zhang, J.; Chan, Y.; Loh, K. P. *Adv. Funct. Mater.* **2014**, *24*, 1904.

(18) Shen, H.; Zheng, Y.; Wang, H.; Xu, W.; Qian, L.; Yang, Y.; Titov, A.; Hyvonen, J.; Li, L. S. *Nanotechnology* **2013**, *24*, No. 475603.

(19) Nanda, J.; Ivanov, S. A.; Achermann, M.; Bezel, I.; Piryatinski, A.; Klimov, V. I. *J. Phys. Chem. C* **2007**, *111*, 15382.

(20) Lin, C. H.; Yang, R. Q.; Zhang, D.; Murry, S. J.; Pei, S. S.; Allerman, A. A.; Kutz, S. R. *Electron. Lett.* **1997**, *33*, 598.

(21) Groeneveld, E.; van Berkum, S.; van Schooneveld, M. M.; Gloter, A.; Meeldijk, J. D.; van den Heuvel, D. J.; Gerritsen, H. C.; de Mello Donega, C. *Nano Lett.* **2012**, *12*, 749.

(22) Kumar, S.; Jones, M.; Lo, S. S.; Scholes, G. D. *Small* **2007**, *3*, 1633.

(23) Joo, J.; Son, J. S.; Kwon, S. G.; Yu, J. H.; Hyeon, T. *J. Am. Chem. Soc.* **2006**, *128*, 5632.

(24) Liu, Y.-H.; Wayman, V. L.; Gibbons, P. C.; Loomis, R. A.; Buhro, W. E. *Nano Lett.* **2010**, *10*, 352.

(25) Son, J. S.; Wen, X.-D.; Joo, J.; Chae, J.; Baek, S.-i.; Park, K.; Kim, J. H.; An, K.; Yu, J. H.; Kwon, S. G.; Choi, S.-H.; Wang, Z.; Kim, Y.-W.; Kuk, Y.; Hoffmann, R.; Hyeon, T. *Angew. Chem., Int. Ed.* **2009**, *48*, 6861.

(26) Li, Z.; Peng, X. *J. Am. Chem. Soc.* **2011**, *133*, 6578.

(27) Ithurria, S.; Tessier, M. D.; Mahler, B.; Lobo, R. P. S. M.; Dubertret, B.; Efros, A. L. *Nat. Mater.* **2011**, *10*, 936.

(28) Li, Z.; Qin, H.; Guzun, D.; Benamara, M.; Salamo, G.; Peng, X. *Nano Res.* **2012**, *5*, 337.

(29) Bouet, C.; Mahler, B.; Nadal, B.; Abecassis, B.; Tessier, M. D.; Ithurria, S.; Xu, X.; Dubertret, B. *Chem. Mater.* **2013**, *25*, 639.

(30) Pedetti, S.; Nadal, B.; Lhuillier, E.; Mahler, B.; Bouet, C.; Abécassis, B.; Xu, X.; Dubertret, B. *Chem. Mater.* **2013**, *25*, 2455.

(31) Mahler, B.; Nadal, B.; Bouet, C.; Patriarche, G.; Dubertret, B. *J. Am. Chem. Soc.* **2012**, *134*, 18591.

(32) Ithurria, S.; Talapin, D. V. *J. Am. Chem. Soc.* **2012**, *134*, 18585.

(33) Tessier, M. D.; Mahler, B.; Nadal, B.; Heuclin, H.; Pedetti, S.; Dubertret, B. *Nano Lett.* **2013**, *13*, 3321.

(34) Prudnikau, A.; Chuvilin, A.; Artemyev, M. *J. Am. Chem. Soc.* **2013**, *135*, 14476.

(35) Tessier, M. D.; Spinicelli, P.; Dupont, D.; Patriarche, G.; Ithurria, S.; Dubertret, B. *Nano Lett.* **2014**, *14*, 207.

(36) Lhuillier, E.; Robin, A.; Ithurria, S.; Aubin, H.; Dubertret, B. *Nano Lett.* **2014**, *14*, 2715.

(37) Lhuillier, E.; Pedetti, S.; Ithurria, S.; Heuclin, H.; Nadal, B.; Robin, A.; Patriarche, G.; Lequeux, N.; Dubertret, B. *ACS Nano* **2014**, *8*, 3813.

(38) Ithurria, S.; Bousquet, G.; Dubertret, B. *J. Am. Chem. Soc.* **2011**, *133*, 3070.

(39) Kim, Y. D.; Klein, M. V.; Ren, S. F.; Chang, Y. C.; Luo, H.; Samarth, N.; Furdyna, J. K. *Phys. Rev. B* **1994**, *49*, 7262.

(40) Wei, S.-H.; Zhang, S. B.; Zunger, A. *J. Appl. Phys.* **2000**, *87*, 1304.

(41) de Mello Donegá, C. *Phys. Rev. B* **2010**, *81*, No. 165303.

(42) Schmitt-Rink, S.; Miller, D. A.; Chemla, D. S. *Phys. Rev. B* **1987**, *35*, 8113.

(43) Groeneveld, E.; de Mello Donegá, C. *J. Phys. Chem. C* **2012**, *116*, 16240.

(44) Marcus, R. A.; Sutin, N. *Biochim. Biophys. Acta* **1985**, *811*, 265.

(45) Scholes, G. D.; Jones, M.; Kumar, S. *J. Phys. Chem. C* **2007**, *111*, 13777.

(46) Zhang, W.; Chen, G.; Wang, J.; Ye, B.-C.; Zhong, X. *Inorg. Chem.* **2009**, *48*, 9723.

(47) Benchamekh, R.; Gippius, N. A.; Even, J.; Nestoklon, M. O.; Jancu, J. M.; Ithurria, S.; Dubertret, B.; Efros, A. L.; Voisin, P. *Phys. Rev. B* **2014**, *89*, No. 035307.

(48) Achtstein, A. W.; Schliwa, A.; Prudnikau, A.; Hardzei, M.; Artemyev, M. V.; Thomsen, C.; Woggon, U. *Nano Lett.* **2012**, *12*, 3151.

(49) Ivanov, S. A.; Piryatinski, A.; Nanda, J.; Tretiak, S.; Zavadil, K. R.; Wallace, W. O.; Werder, D.; Klimov, V. I. *J. Am. Chem. Soc.* **2007**, *129*, 11708.

(50) Cragg, G. E.; Efros, A. L. *Nano Lett.* **2010**, *10*, 313.

(51) Bailey, R. E.; Nie, S. *J. Am. Chem. Soc.* **2003**, *125*, 7100.

(52) Poon, H. C.; Feng, Z. C.; Feng, Y. P.; Li, M. F. *J. Phys.: Condens. Matter* **1995**, *7*, 2783.

(53) Vegard, L. *Z. Phys.* **1921**, *5*, 17.
(54) Kaniyankandy, S.; Rawalekar, S.; Ghosh, H. N. *J. Mater. Chem. C* **2013**, *1*, 2755.
(55) Oron, D.; Kazes, M.; Banin, U. *Phys. Rev. B* **2007**, *75*, No. 035330.
(56) Jones, M.; Kumar, S.; Lo, S. S.; Scholes, G. D. *J. Phys. Chem. C* **2008**, *112*, 5423.
(57) Yang, Y. A.; Wu, H.; Williams, K. R.; Cao, Y. C. *Angew. Chem., Int. Ed.* **2005**, *44*, 6712.
(58) García-Rodríguez, R.; Liu, H. *J. Am. Chem. Soc.* **2012**, *134*, 1400.